Original Research

Machine learning–based prediction of heat pain sensitivity by using resting-state EEG

Fu-Jung Hsiao[1,*], Wei-Ta Chen[1,2,3,4,*], Li-Ling Hope Pan[1], Hung-Yu Liu[2,3], Yen-Feng Wang[2,3], Shih-Pin Chen[1,2,3], Kuan-Lin Lai[2,3], Shuu-Jiun Wang[1,2,3]

[1]*Brain Research Center, National Yang-Ming Chiao-Tung University, 11221 Taipei, Taiwan,* [2]*School of Medicine, National Yang-Ming Chiao-Tung University, 11221 Taipei, Taiwan,* [3]*Department of Neurology, Neurological Institute, Taipei Veterans General Hospital, 11217 Taipei, Taiwan,* [4]*Department of Neurology, Keelung Hospital, Ministry of Health and Welfare, 20147 Keelung, Taiwan*

TABLE OF CONTENTS

1. Abstract

Introduction: The development of quantitative, objective signatures or predictors to evaluate pain sensitivity is crucial in the clinical management of pain and in precision medicine. This study combined multimodal (neurophysiology and psychometrics) signatures to classify the training dataset and predict the testing dataset on individual heat pain sensitivity. **Methods**: Healthy individuals were recruited in this study. Individual heat pain sensitivity and psychometric scores, as well as the resting-state electroencephalography (EEG) data, were obtained from each participant. Participants were divided into low-sensitivity and high-sensitivity subgroups according to their heat pain sensitivity. Psychometric data obtained from psychometric measurements and power spectral density (PSD) and functional connectivity (FC) derived from resting-state EEG analysis were subjected to feature selection with an independent *t* test and were then trained and predicted using machine learning models, including support vector machine (SVM) and k-nearest neighbor. **Results**: In total, 85 participants were recruited in this study, and their data were

Submitted: 9 September 2021 Revised: 22 November 2021 Accepted: 24 November 2021 Published: 30 December 2021

divided into training (n = 65) and testing (n = 20) datasets. We identified the resting-state PSD and FC, which can serve as brain signatures to classify heat pain as high-sensitive or low-sensitive. Using machine learning algorithms of SVM with different kernels, we obtained an accuracy of 86.2%–93.8% in classifying the participants into thermal pain high-sensitivity and low-sensitivity groups; moreover, using the trained model of cubic SVM, an accuracy of 80% was achieved in predicting the pain sensitivity of an independent dataset of combined PSD and FC features of resting-state EEG data. **Conclusion**: Acceptable accuracy in classification and prediction by using the SVM model indicated that pain sensitivity could be achieved, leading to considerable possibilities of the use of objective evaluation of pain perception in clinical practice. However, the predictive model presented in this study requires further validation by studies with a larger dataset.

2. Introduction

The International Association for the Study of Pain defined pain as "an unpleasant sensory and emotional experience associated with, or resembling that associated with, actual or potential tissue damage" [1]. In addition, pain is a subjective perceptual phenomenon that is determined by biological, psychological, and social factors. Therefore, quantitative characterization of pain sensitivity may have significant clinical utility in predicting responses to a clinical procedure [2]. Moreover, accumulated evidence suggests that altered pain sensitivity was associated with Alzheimer disease [3, 4], Parkinson disease [5], fibromyalgia [6], and migraine and tension-type headache [7]. Self-reported quantitative sensory testing is the gold standard in pain sensitivity measurement [8]. Thus, research focused on the development of quantitative predictors to aid the evaluation of pain sensitivity is of increasing importance in the clinical management of pain and in precision medicine.

Studies have suggested that pain sensitivity was associated with neuronal activities and multiple functional brain networks. The rating of individual pain using noxious stimulation was linked to cortical activation [9–12], and pain intensity to heat stimuli was related to gamma oscillation in the medial frontal cortex [12]. In previous studies, during capsaicin-heat pain stimulation, peak alpha frequency over the sensorimotor region was inversely correlated with individual pain intensity [11, 13]. In our recent study, we further confirmed that pain sensitivity is associated with the spontaneous regional oscillatory activities and intrinsic functional network [14]. Taken together, these findings suggest that cortical activation and functional network may reflect individual pain sensitivity and cause individual differences in pain perception. Although neural correlates of pain sensitivity have been investigated, whether these brain signatures could be used to predict individual pain sensitivity remains elusive.

Machine learning involves the use of an algorithm to automatically detect patterns in data and then predict or classify future data; thus, it learns from data without the need for previous knowledge and aims at optimizing the performance of the model. In pain research applications, machine learning uses pain-related data for feature mapping; learning the signatures of pain conditions, types, or disorders; and constructing the prediction model, which can be applied to new data to identify or predict pain phenotypes. In the past decade, machine learning has been used to assess pain elicited by noxious heat in healthy persons with fine performance (85–94% sensitivity and 73–94% specificity) using functional magnetic resonance imaging (MRI) data [15], and classify pain and nonpain conditions with an accuracy of 81% by using whole-brain activities obtained from functional MRI data [16], high and low pain intensities with an accuracy of 86.3% by using laser-evoked potential from electroencephalography (EEG) data [17], baseline and pain threshold conditions with an accuracy of 79.29% by using facial electromyography data [18], and healthy individuals and patients with migraine with an accuracy of 91.4% and 88.7% by using resting-state data of functional MRI [19] and somatosensory evoked potentials of EEG, respectively [20]. As a result, machine learning might have a great potential to predict individual pain sensitivity from pain-related neurophysiological or psychological data.

As resting-state brain activities were associated with individual pain sensitivity in our recent study [14], spontaneous cortical oscillations and intrinsic functional networks might be pivotal mechanisms in the regulation of pain processes. Therefore, this study combined multimodal (neurophysiology and psychometrics) signatures, which might better represent pain complexity, and built a multivariate machine-learning model, which learns from the features of psychometric scores (from demography and questionnaires), spontaneous brain oscillatory powers (from within-electrode EEG analysis), and resting-state functional connectivity (FC, from between-electrode EEG analysis), to noticeably classify the training dataset and predict the testing dataset on individual heat pain sensitivity derived from the heat pain threshold (HPT).

3. Materials and methods

3.1 Participants

This study recruited healthy individuals who did not have a medical or family history of pain disorders and had not experienced any significant pain condition during the past year. All participants were right-handed, denied having any history of systemic or major neuropsychiatric disease, and had normal physical and neurological examination results as well as normal brain MRI results. Participants taking any medication on a daily basis were excluded. All participants underwent scheduled pain sensitivity mea-

surements and EEG recordings, and their degrees of psychometric factors were assessed (detailed in 3.2 and 3.3).

The Institutional Review Board of National Yang-Ming University approved the study protocol (YM108044F), and each participant provided written informed consent.

3.2 HPT and psychometric measurements

Pain sensitivity measurement was obtained in the pain examination room (with a constant room temperature of 20 °C and no windows) in the Department of Neurology at Taipei Veterans General Hospital. Quantitative measurements of HPT were defined as the lowest intensity perceived as painful for participants, and HPT values were obtained as follows. Standardized instructions were provided to all participants before obtaining the measurements. Each participant received HPT measurements at the left forehead by using the Medoc Pathway platform (TSA-II, Medoc Ltd. Advanced Medical Systems, Ramat Yishai, Israel) with a thermode (30 mm × 30 mm), which provided an absolute temperature accuracy of ±0.3 °C, temperature repeatability of ±0.2 °C, and a set-Point resolution of 0.1 °C. The thermode was applied to the skin and fastened with a hook and loop strap. Using the stimulation method of limits, the temperature of thermode was increased at a rate of 1 °C/sec from its starting point at 32 °C until the participant pressed a button to indicate that the stimulus became painful. Testing was performed five times, and the mean of all trials was considered the pain threshold of the participant. On the basis of HPT values, participants were divided into low-sensitive and high-sensitive groups. Low-sensitivity was defined as HPT more than the median HPT value of all participants, and high-sensitivity was defined as HPT less than or equal to the median HPT value of all participants.

Regarding psychometric measurements, we evaluated sleep efficiency (in %) derived from the ratio of the total sleep time to time in bed (multiplied by 100 to yield a percentage) using the Pittsburgh Sleep Quality Index (PSQI); the extent of catastrophic thinking due to pain according to three components, namely rumination, magnification, and helplessness, determined using the Pain Catastrophizing Scale (PCS); the degree to which the participants appraised situations in their lives as stressful on the Perceived Stress Scale; anxiety and depression by using the Hospital Anxiety and Depression Scale (HADS); and the quantification of stress by analyzing life events using Recent Life Changes Questionnaire.

3.3 Resting-state EEG recording and analysis

EEG recording (Brain Products GmbH, Munich, Germany) was conducted for 5 min with a digitization rate of 1000 Hz; participants were instructed to close their eyes but remain awake and relaxed and perform no explicit task, which eliminated the artifacts of eye movement and revealed that the intrinsic cortical activities were associated with pain sensitivity in our recent study [14]. The recording was stopped and then rerun if a participant fell asleep. All the subjects were asked not to consume caffeine 48 h before the EEG assessment [21]. Electrooculography activity was simultaneously acquired for offline artefact elimination. Scalp EEG was collected from an EEG cap housing a 64-electrode BrainVision actiCAP system, which covered the whole brain according to the extended international 10–20 system [22]. Active circuits for impedance conversion, achieving outstanding signal quality even with higher impedances compared with conventional passive electrodes, are integrated directly in the actiCAP slim electrodes. All electrodes were referenced online to an electrode placed at the Fz and a common ground set at the FPz site. The EEG signal was amplified and digitized using a BrainAmp DC amplifier linked to Brain Vision Recorder software (version 2.1, Brain Products GmbH, Munich, Germany).

In the preprocessing stage, a bandpass filter of 1–40 Hz was applied to all data to remove the DC drift and 60-Hz power noise. Then, to eliminate nonbrain artefacts from the resting-state EEG data, apparent eye contaminations were manually removed through visual inspection; moreover, identified heartbeat and eye blinking events from electro-cardiographic and electro-oculographic data were used to define the projectors through principal component analysis separately. The principal components meeting the artifact's sensor topography were then manually excluded through orthogonal projection [23]. To obtain the electrode-based resting-state oscillations and FC, the spontaneous activities of each electrode were further analyzed as follows [14, 24–26]. First, oscillatory power in each electrode was estimated using the Welch method (window duration: 3 sec with 50% overlap) and defined as absolute power spectral density (PSD). Moreover, the oscillatory power was spectrally normalized through the division of power at each frequency band by the total power, which adequately reduce the interindividual variability of the oscillatory magnitude [27]. Second, the amplitude envelope correlation analysis [28], which orthogonalized the signals to remove zero-lag interactions [29], was used to calculate the FC between electrodes and then the full 63 × 63 adjacency matrix was constructed for each frequency band. Amplitude envelope correlation analysis is briefly described as follows. The time-varying dynamics of bandpass filtered electrical activity of each electrode were Hilbert transformed to obtain the analytic signal. The absolute value of the analytic signal was then determined in order to give the envelope of oscillatory power in the frequency band of interest. The Hilbert envelopes for the EEG data were divided into N time segments of equal length (3 seconds in this study). The Pearson correlation coefficient between electrodes and Hilbert envelopes was computed within each segment. This gave N correlation values, one for each time segment. These were then averaged across segments yielding a single av-

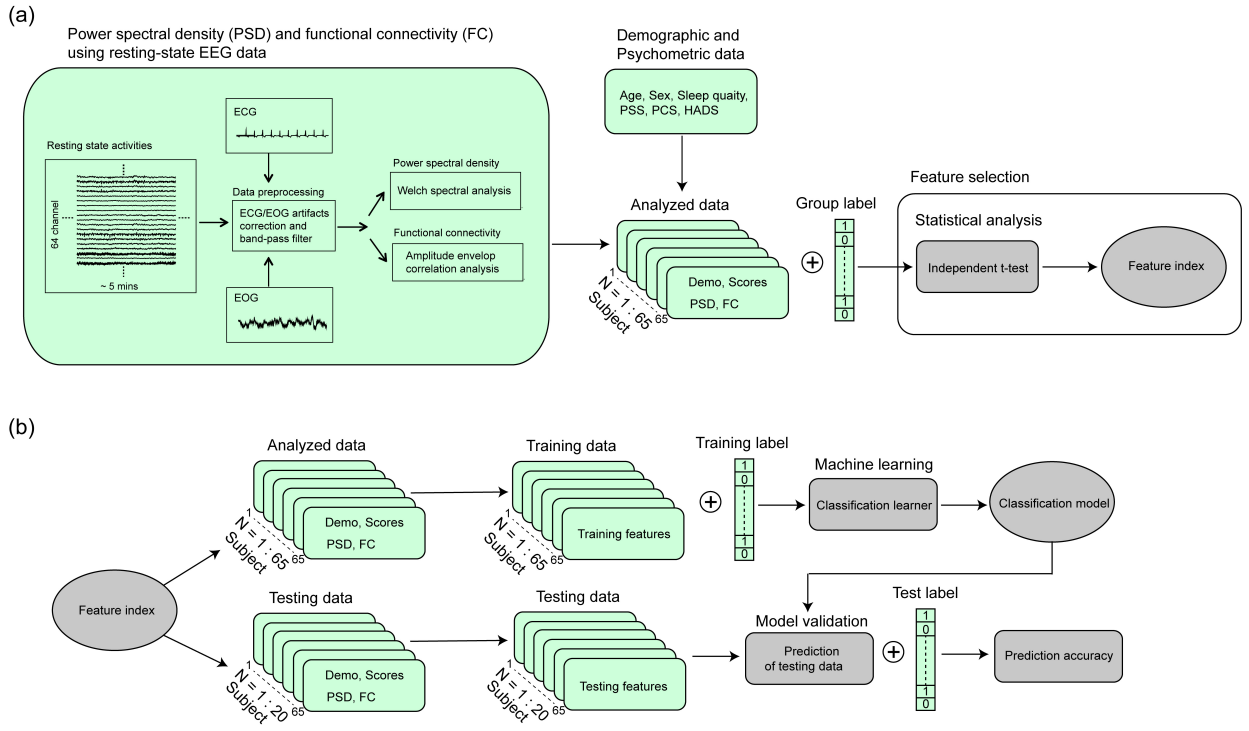

Fig. 1. Pipeline of data processing and machine learning model. (a) Feature extraction of resting-state EEG data and feature selection from demographic, psychometric, and neurophysiological data. (b) Classification using training dataset and validation using testing dataset. PSS, perceived stress scale; PCS, pain catastrophizing scale; HADS, hospital anxiety and depression scale. Demo, demographic data.

erage value which was termed Averaged Envelope Correlation (for a mathematical description see [30]). Oscillatory power and FC were categorized according to the following frequency bands and averaged in each frequency range: delta (2–4 Hz), theta (5–7 Hz), alpha (8–13 Hz), beta (14–25 Hz), and gamma (26–40 Hz). EEG data preprocessing and analysis were performed using Brainstorm [31].

3.4 Feature extraction and selection

On the basis of prior findings, which suggested that pain perception is associated with central modulation; distributed cortical involvement; and the interaction of sensory, cognitive and affective processes, multimodal signatures including the psychometric data (Psy) and functional EEG activities within and between brain regions would accurately manifest the underlying neurophysiological mechanism. Thus, the extraction of these features is desirable to establish the predictive model and obtain high classification accuracy. In our study, all individual's data were split into training and testing datasets, and the extracted features were organized in three data types: Psy obtained from psychometric measurements, and PSD and FC derived from resting-state EEG analysis (Fig. 1).

Feature selection is a process of selecting a subset of features from the original set of extracted features to increase the classification performance with a compact feature subset, which might reduce computational complexity and diminish irrelevant features. Therefore, we applied a feature selection procedure by using the univariate analysis (independent t test) for the high-sensitivity versus low-sensitivity factor to obtain the most discriminative features for classification (Fig. 1). In this study, for Psy and PSD, the feature index with significant difference between groups ($p < 0.05$) was selected for their discriminative characteristics; moreover, for FC, the discriminative feature index was decided from the significant group difference (uncorrected $p < 0.005$). Thus, the discriminative features of Psy, PSD, and FC were used to construct training and testing datasets.

3.5 Performance evaluation of classification models

The kernel functions and parameters for all classification analyses are listed in Table 1. To avoid the overfitting problem, model training processes were based on a five-fold leave-one-out cross-validation technique, which were unbiased in the sense that the training features were selected from each test case. The performance of each classification model was evaluated based on accuracy, sensitivity, and specificity, as well as the area under the receiver operating characteristics curve (AUC). Here, sensitivity and specificity represent the proportion of low-sensitive and high-sensitive participants, respectively, correctly classified.

After the reconstruction and evaluation of classification models from the training dataset, these models were further validated to determine whether identified features can be generalizable across different populations. First, the

Table 1. Models and parameters of machine classification.

SVM	Kernel function	Kernel scale
Linear SVM	Linear	auto
Quadratic SVM	Quadratic	auto
Cubic SVM	Cubic	auto
Fine Gaussian SVM	Gaussian	3
Medium Gaussian SVM	Gaussian	12
Coarse Gaussian SVM	Gaussian	48
KNN	No. of neighbors	Distance weight
Fine KNN	1	equal
Medium KNN	10	equal
Coarse KNN	100	equal
Cosine KNN	10	equal
Cubic KNN	10	equal
Weighted KNN	10	squared inverse

SVM, support vector machine; KNN, K-nearest neighbor; No., number.

testing dataset was correspondingly applied to preprocessing and analysis, and then feature selection was performed based on the discriminative feature index from the training dataset. The discriminative features of Psy, PSD, and FC in the testing dataset were used in the trained classification models to differentiate between participants with low-sensitivity and high-sensitivity. The labels of the testing dataset were blinded, and the classification models were applied to the discriminative features without any model training procedure. The predictive accuracy and AUC were obtained for each model. Additionally, to estimate the statistical significance of predictive accuracy, statistical significance of the observed classification accuracy was estimated using nonparametric permutation tests (1000 times).

4. Results

4.1 Demographic and psychometric data

This study included 85 healthy participants who were divided into high-sensitivity (n = 43) and low-sensitivity (n = 42) groups according certain criteria. Demographic and psychometric profiles are summarized in Table 2. The groups did not differ significantly in terms of age, sex, height, or weight. In terms of the psychometric data, sleep efficiency, perceived stress, and recent life changes were similar between groups. However, pain catastrophizing (PCS), anxiety (HADS_A), and depression (HADS_D) scores were higher in the high-sensitivity group than in the low-sensitivity group (all $p < 0.05$). Notably, the HPT of all participants is 43.1 $\pm$ 3.5 °C and the median value is 43.4 °C. The demographic, psychometric and EEG data from the last 10 subjects of each group were selected as the testing dataset; therefore, all data were divided into training (n = 65) and testing (n = 20) datasets (Fig. 1). Notably, in the training dataset (n = 65), differences between groups were noted for PCS, HADS_A, and HADS_D scores. Consequently, these three scores were selected as the discriminative features of psychometric scores (Psy type) for further classification.

Table 2. Demographics and Psychometric data.

	Group		*p*-value
	High-sensitivity	Low-sensitivity	
N	43	42	
Demographics			
Age (years)	28.6 $\pm$ 7.2	30.1 $\pm$ 8.3	0.393
Gender	24F/19M	25F/17M	0.827
Height (cm)	166.3 $\pm$ 8.8	166.6 $\pm$ 7.7	0.829
Weight (kg)	65.5 $\pm$ 14.4	62.7 $\pm$ 12.2	0.326
Clinical scores			
EFF (%)	91.3 $\pm$ 8.0	89.1 $\pm$ 11.1	0.292
PCS	7.5 $\pm$ 7.8	4.4 $\pm$ 5.1	0.032*
PSS	23.7 $\pm$ 7.8	21.0 $\pm$ 7.7	0.11
HADS_A	4.8 $\pm$ 3.2	2.9 $\pm$ 2.8	0.004**
HADS_D	3.3 $\pm$ 3.2	1.9 $\pm$ 2.0	0.022*
RLCQ	162.9 $\pm$ 147.0	128.6 $\pm$ 133.5	0.263
HPT	40.4 $\pm$ 2.1	46.1 $\pm$ 2.0	<0.001**

High-sensitivity, Low heat pain threshold; Low-sensitivity, High heat pain threshold; F, Female; M, Male; EFF, Sleep efficiency; PCS, Pain catastrophizing score; PSS, Perceived stress scale; HADS, Hospital anxiety and depression score; A, Anxiety; D, Depression; RLCQ, Recent life changes questionnaire; HPT, Heat pain threshold. *$p < 0.05$; **$p < 0.01$.

4.2 Feature selection of resting-state EEG

The spatial distribution of spectral power in high-sensitivity and low-sensitivity groups and differences in the statistical topographic mappings of PSD between high-sensitivity and low-sensitivity groups in different frequency bands are illustrated in Fig. 2. Regarding the absolute PSD (Fig. 2a), in the alpha, beta, and gamma bands, larger spectral powers were observed in the high-sensitivity group than in the low-sensitivity group ($p < 0.05$), indicating that individuals with pain high-sensitivity have augmented spontaneous oscillations. In total, 12 electrodes exhibited a group difference and were mainly located over the frontal, fronto-temporal, and central regions. For the normalized PSD (Fig. 2b), in the delta and theta bands, smaller spectral powers were noted in the high-sensitivity group than in the low-sensitivity group ($p < 0.05$), whereas in the alpha, beta, and gamma bands, spectral powers were higher in the high-sensitivity group than in the low-sensitivity group ($p < 0.05$). In total, 70 features with significant power differences were widely distributed over the frontal, fronto-temporal, parietal, central, and occipital regions. These 70 features of normalized PSD and 12 features of absolute PSD values were selected as the discriminative features of PSD for further classification.

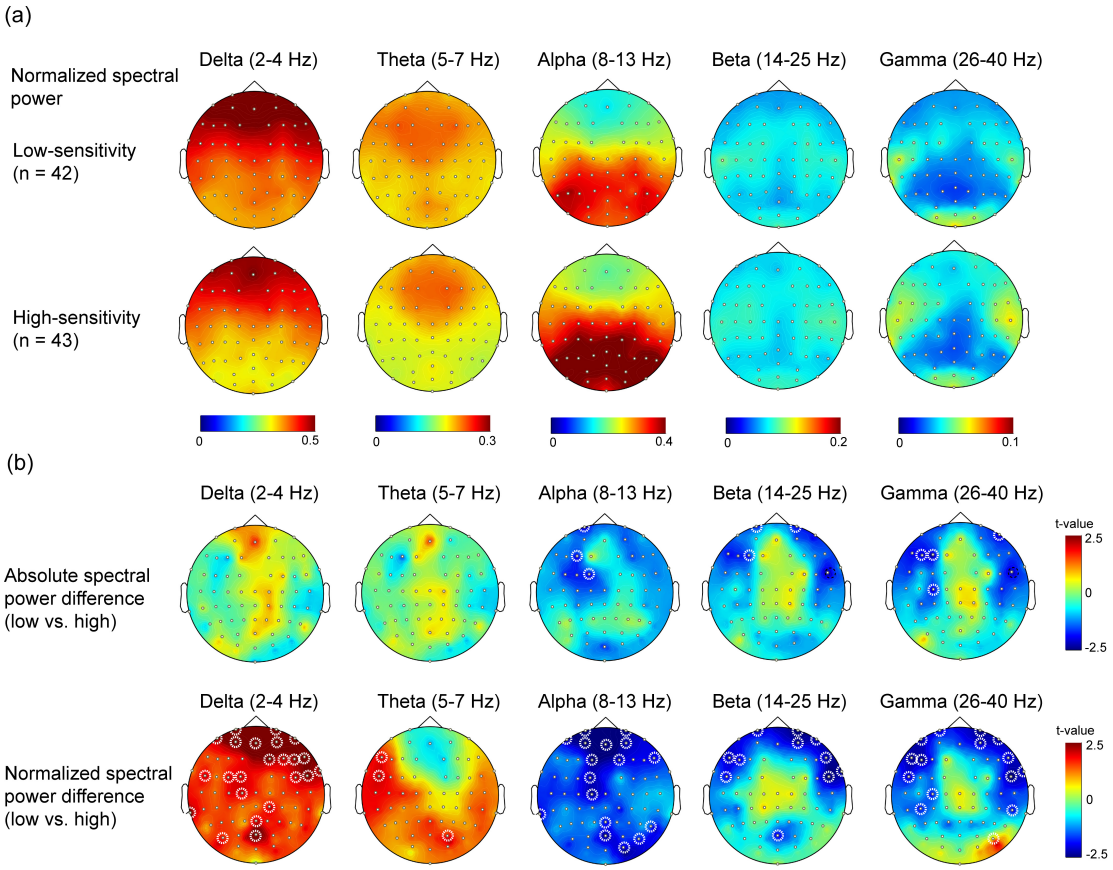

Fig. 2. Power spectral density between groups. (a) Normalized spectral power density in low-sensitivity and high-sensitivity groups. (b) Difference of absolute and normalized power spectral density between subjects with low- and high-sensitivity. Dashed circle indicates the electrode with significant difference between groups ($p < 0.05$). High, high-sensitivity; Low, low-sensitivity.

Differences in resting-state FC between groups are statistically illustrated with adjacency matrices from delta to gamma bands (Fig. 3a). In general, decreased FC values in the high-sensitivity group in delta, theta, beta, and gamma bands were observed between specific connections in comparison with those in the low-sensitivity group, indicating that decreased oscillatory connectivity characterized the intrinsic functional connections in participants with high-sensitivity. By contrast, increased alpha FC values were noted in participants with high-sensitivity. Fig. 3b shows the consensus map of discriminative features, which represents the significant difference between groups ($p < 0.0005$). The ring coded in gray level exhibits the number of occurrences for each electrode in the consensus map. In total, 145 discriminative features (FC type) were selected for further classification.

4.3 Classification using discriminative features of training dataset

Using one type of discriminative feature (Psy, PSD, or FC), the performance of models with different kernel functions for each type of input features is shown in Fig. 4. With Psy, the best model (fine Gaussian support vector machine [SVM]) among all training models had an accuracy of 55.4% and AUC of 0.63. With PSD, the best model (medium Gaussian SVM) had an accuracy of 73.8% and AUC of 0.79. With FC, the best models (accuracy >85%) included the linear (accuracy = 87.7%, AUC = 0.96), quadratic (accuracy = 92.3%, AUC = 0.96) and cubic (accuracy = 92.3%, AUC = 0.96) SVMs. These models were further evaluated using the testing dataset.

Using a combination of two types of discriminative features, the classification performance was also examined in the training process (Fig. 5). Using the combination of Psy and PSD (total 85 features), coarse Gaussian SVM achieved the best accuracy of 73.8% and AUC of 0.79. As for the combination of Psy and FC (148 features), linear (accuracy = 90.8%, AUC = 0.97), quadratic (accuracy = 93.8%, AUC = 0.97), and cubic (accuracy = 92.3%, AUC = 0.96) SVM had the finest performance. For the combination of PSD and FC (227 features), the classification exhibited the accuracy of >85% and AUC of >0.9 using linear, quadratic, cubic, medium Gaussian, and coarse Gaussian SVM models. Moreover, these nine models were further validated using the testing dataset.

The performance of the combination of all three types of discriminative features (total 230 features) was investigated using the training dataset (Fig. 6). SVM model

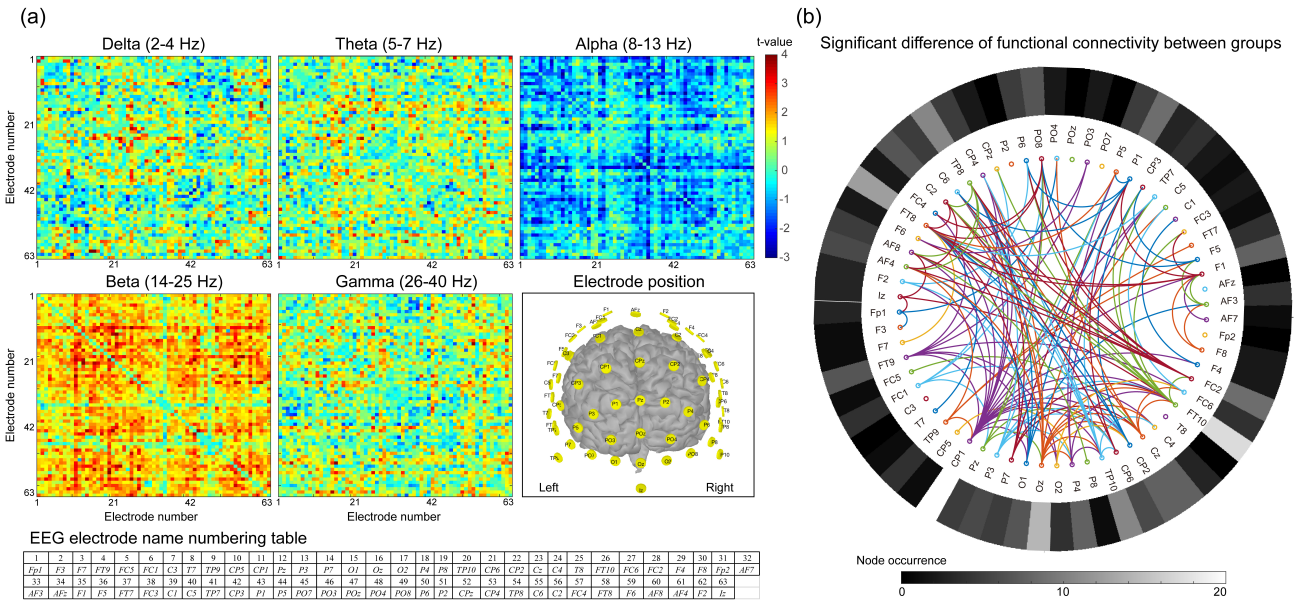

1	2	3	4	5	6	7	8	9	10	11	12	13	14	15	16	17	18	19	20	21	22	23	24	25	26	27	28	29	30	31	32
Fp1	*F3*	*F7*	*FT9*	*FC5*	*FC1*	*C3*	*T7*	*TP9*	*CP5*	*CP1*	*Pz*	*P3*	*P7*	*O1*	*Oz*	*O2*	*P4*	*P8*	*TP10*	*CP6*	*CP2*	*Cz*	*C4*	*T8*	*FT10*	*FC6*	*FC2*	*F4*	*F8*	*Fp2*	*AF7*
33	34	35	36	37	38	39	40	41	42	43	44	45	46	47	48	49	50	51	52	53	54	55	56	57	58	59	60	61	62	63	
AF3	*AFz*	*F1*	*F5*	*FT7*	*FC3*	*C1*	*C5*	*TP7*	*CP3*	*P1*	*P5*	*PO7*	*PO3*	*POz*	*PO4*	*PO8*	*P6*	*P2*	*CPz*	*CP4*	*TP8*	*C6*	*C2*	*FC4*	*FT8*	*F6*	*AF8*	*AF4*	*F2*	*Iz*	

Fig. 3. Functional connectivity between groups. (a) Statistical difference of electrode–electrode functional connectivity in each frequency band between participants with low- and high-sensitivity. Electrode position illustrates the arrangement of each electrode. The table shows the electrode name corresponding to each number. (b) The consensus map exhibits the significant functional connectivity difference between subjects with low- and high-sensitivity ($p < 0.005$). Node occurrence displays the connections with significance from this electrode.

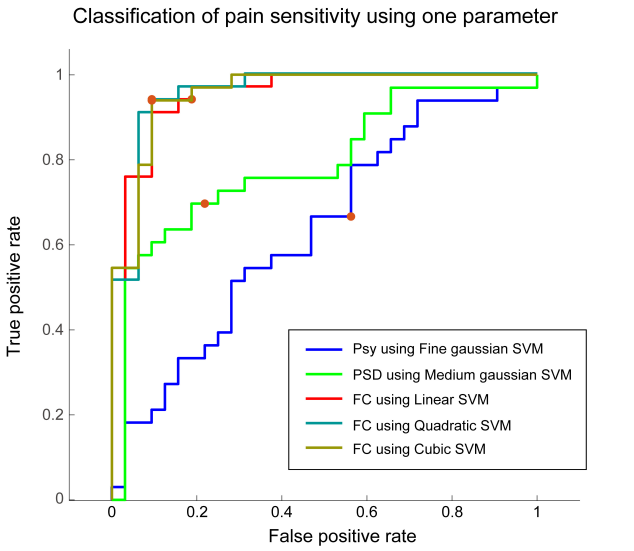

Type	Features	Model	Accuracy(%)	Sensitivity	Specificity	AUC
Psy	3	Fine gaussian SVM	55.4	0.44	0.67	0.63
PSD	82	Medium gaussian SVM	73.8	0.78	0.7	0.79
FC	145	Linear SVM	**87.7**	0.81	0.94	0.96
FC	145	Quadratic SVM	**92.3**	0.91	0.94	0.96
FC	145	Cubic SVM	**92.3**	0.91	0.94	0.96

Fig. 4. Classification using one type of features. Model performance using psychometric, PSD, or FC features. Psy, psychometric data; PSD, power spectral density; FC, functional connectivity; SVM, support vector machine; AUC, area under the curve.

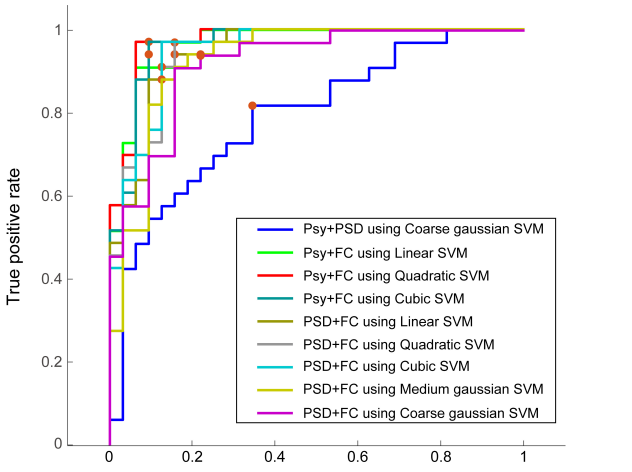

Type	Features	Model	Accuracy(%)	Sensitivity	Specificity	AUC
Psy+PSD	85	Coarse gaussian SVM	73.8	0.66	0.82	0.79
Psy+FC	148	Linear SVM	**90.8**	0.84	0.97	0.97
Psy+FC	148	Quadratic SVM	**93.8**	0.91	0.97	0.97
Psy+FC	148	Cubic SVM	**92.3**	0.91	0.94	0.96
PSD+FC	227	Linear SVM	**89.2**	0.84	0.94	0.95
PSD+FC	227	Quadratic SVM	**89.2**	0.84	0.88	0.95
PSD+FC	227	Cubic SVM	**87.7**	0.84	0.88	0.95
PSD+FC	227	Medium gaussian SVM	**86.2**	0.78	0.94	0.93
PSD+FC	227	Coarse Gaussian SVM	**86.2**	0.78	0.94	0.92

Fig. 5. Classification using two types of features. Model performance using combined features using two of psychometric, PSD, or FC. Psy, psychometric data; PSD, power spectral density; FC, functional connectivity; SVM, support vector machine; AUC, area under the curve.

achieved an accuracy of >85% and AUC of >0.9 by using the kernel functions of linear, quadratic, cubic, medium Gaussian, and coarse Gaussian. In addition, the k-nearest neighbor (KNN) model had an accuracy of >85% and AUC of >0.9 by using medium, cubic, and weighted functions. For further validation by using the testing dataset, these eight models were used as predictive classifiers.

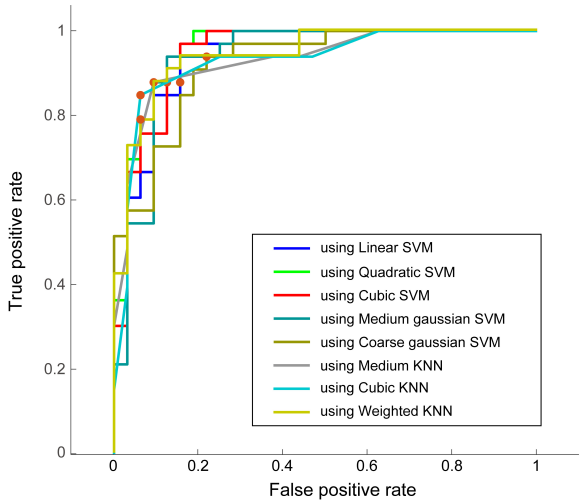

Type	Features	Model	Accuracy(%)	Sensitivity	Specificity	AUC
PSD+Psy+FC	230	Linear SVM	**86.2**	0.84	0.88	0.95
PSD+Psy+FC	230	Quadratic SVM	**87.7**	0.84	0.88	0.93
PSD+Psy+FC	230	Cubic SVM	**87.7**	0.84	0.88	0.93
PSD+Psy+FC	230	Medium Gaussian SVM	**86.2**	0.78	0.94	0.91
PSD+Psy+FC	230	Coarse Gaussian SVM	**86.2**	0.78	0.94	0.92
PSD+Psy+FC	230	Medium KNN	**89.2**	0.91	0.88	0.93
PSD+Psy+FC	230	Cubic KNN	**89.2**	0.94	0.85	0.93
PSD+Psy+FC	230	Weighted KNN	**86.2**	0.94	0.79	0.94

Fig. 6. Classification using all three features. Model performance using psychometric, PSD, and FC features. Psy, psychometric data; PSD, power spectral density; FC, functional connectivity; SVM, support vector machine; AUC, area under the curve.

4.4 Validation of classification models in testing dataset

We further tested the generalizability of the discriminative features and trained models by using a testing dataset of 10 high-sensitive participants and 10 low-sensitive participants. Between groups, no clear difference was observed for the factors of age (high: 28.7 ± 9.6 years, low: 27.6 ± 8.3 years), gender (high: 6F/4M, low: 5F/5M), height (high: 164.3 ± 8.8 cm, low: 168.3 ± 8.8 cm), weight (high: 59.1 ± 10.0 kg, low: 65.3 ± 13.6 kg), sleep efficiency (high: 90.6 ± 6.9, low: 88.4 ± 11.2), pain catastrophizing score (high: 7.0 ± 8.5, low: 3.3 ± 6.9), perceived stress score (high: 25.2 ± 7.5, low: 18.9 ± 9.4), and recent life changes questionnaire (high: 126.3 ± 69.0, low: 126.3 ± 94.4); however, anxiety score (high: 5.5 ± 3.0, low: 2.4 ± 2.4; p = 0.021), depression score (high: 4.1 ± 3.3, low: 1.2 ± 1.8; p = 0.026), and HPT (high: 39.7 ± 2.8 °C, low: 45.8 ± 1.4 °C, $p < 0.001$) differed between high-sensitive and low-sensitive participants. Among different feature types and training models, an accuracy of 80% was achieved using cubic SVM with the combined features of PSD and FC or all features from Psy, PSD, and FC (Fig. 7). Specifically, the validation of PSD and FC in cubic SVM revealed a significant level of accuracy (p = 0.001, permutation test). Moreover, the AUC was 0.8 with 70% sensitivity and 90% specificity, indicating good generalizability in a testing dataset.

5. Discussion

In this study, we identified the resting-state oscillations and functional networks that can serve as brain signatures for the classification between patients with high- and low-sensitivity to heat pain. Using the machine learning algorithms of SVM with different kernels, we obtained an accuracy of 86.2%–93.8% in classifying individuals with thermal pain high-sensitivity or low-sensitivity; moreover, using the trained model of the cubic SVM, an accuracy of 80% was achieved in the prediction of the pain sensitivity of an independent dataset consisting of PSD and FC features obtained from resting-state EEG.

5.1 Discriminative features on pain sensitivity

In feature selection, traditional procedures of the independent t test were performed to obtain discriminative features used in classification and validation models. Regarding psychometric scores, individuals with pain high-sensitivity had augmented anxiety and depression scores consistently in prior studies, suggesting a correlation of pain perception threshold with emotional factors [32, 33]. Moreover, heighted PCS was noted in high-sensitive individuals, echoing the notion that catastrophizing might have a significant impact on pain perception [34, 35]. With regards to the features of PSD and FC, differences in oscillatory power and FC distributed among cortical regions had frequency-specific characteristics. This finding was corroborated with oscillations at different frequencies to the routing of information flow of pain processes in the brain [36]. Furthermore, individual pain sensitivity might result from the integration of sensory, affective, and cognitive states, implying that oscillatory connectivity in the multiple functional networks could underpin pain sensitivity [14].

5.2 Types of features in training accuracy

In pain sensitivity classification, using one type of feature, the discriminative features of FC exhibited better accuracy and AUC compared with those of Psy and PSD, indicating FC within multiple networks effectively represent the underlying central pain process mechanism [14]. Moreover, pain sensitivity might involve sensory, affective, and cognitive processes [37]. Features from Psy or PSD could reflect the partial processing of the central pain perceptual mechanism and lead to unsuitable classification of performance. As for the combination of two types of features from psychometrical scores and oscillatory powers, the performance was still unsatisfactory (accuracy of 73.8% and AUC of 0.79), which supported our notion that not the local neuronal oscillatory activities but synchronizations between multiple brain regions were engaged in the underlying mechanism of pain sensitivity. In addition, these findings suggested that emotional factors might not play a dominant role in the regulation of pain sensitivity. Correspondingly, as all the types of features were used in the classification model, the performance was comparable with that

(a)

Accuracy of trained model using testing dataset

Types of features	Model	Accuracy (%)
Psy	Fine gaussian SVM	60
PSD	Medium gaussian SVM	55
FC	Linear SVM	65
FC	Quadratic SVM	65
FC	Cubic SVM	65
Psy+PSD	Coarse gaussian SVM	60
Psy+FC	Linear SVM	65
Psy+FC	Quadratic SVM	65
Psy+FC	Cubic SVM	65
PSD+FC	Linear SVM	70
PSD+FC	Quadratic SVM	75
PSD+FC	Cubic SVM	**80**
PSD+FC	Medium gaussian SVM	65
PSD+FC	Coarse Gaussian SVM	60
PSD+Psy+FC	Linear SVM	70
PSD+Psy+FC	Quadratic SVM	75
PSD+Psy+FC	Cubic SVM	**80**
PSD+Psy+FC	Medium Gaussian SVM	65
PSD+Psy+FC	Coarse Gaussian SVM	60
PSD+Psy+FC	Medium KNN	65
PSD+Psy+FC	Cubic KNN	75
PSD+Psy+FC	Weighted KNN	75

(b)

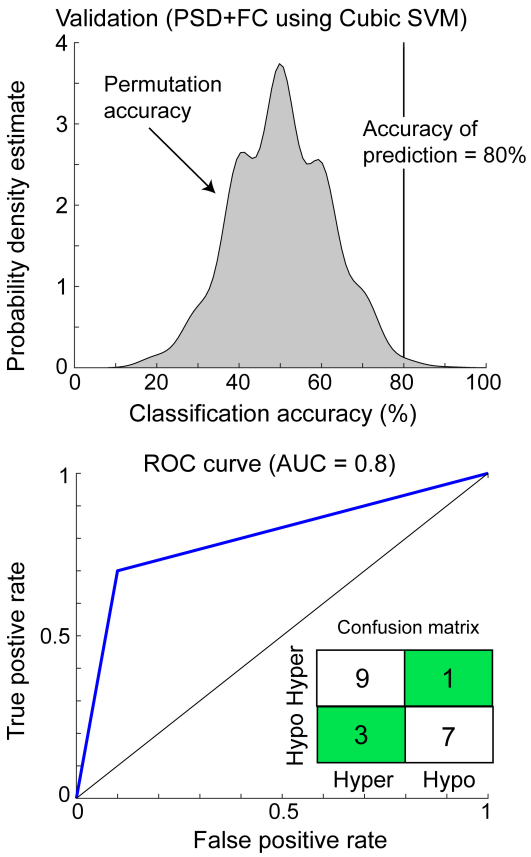

Fig. 7. Validation of trained models using testing dataset. (a) The accuracy of all trained model using independent testing dataset. (b) Permutation test of accuracy (80%) using cubic SVM (p = 0.001) and the receiver operating characteristic curve (ROC) with AUC of 0.8. Psy, psychometric data; PSD, power spectral density; FC, functional connectivity; SVM, support vector machine; KNN, k-nearest neighbor; AUC, area under the curve; low, low-sensitivity; high, high-sensitivity.

of PSD and FC. Notably, in the classification models using two types of features, the SVM model with different kernel functions had satisfactory accuracy and AUC, whereas using all types of features for classification, both SVM and KNN exhibited good performance. These findings could postulate that the SVM model is recommended for establishing the algorithms in identifying pain sensitivity. Taken together, we suggested that pain sensitivity might be classified from the SVM model, particularly using the features of resting-state brain oscillations and FC.

5.3 Validation of classification models

Machine learning is vulnerable to overfitting and may cause confounding with noise or irrelevant features. Hence, in addition to successfully learning the features and classifying the actual data, the models should be used to predict new datasets. Remarkably, in this study, the trained SVM model with PSD and FC features was validated using an independent testing dataset, and the results revealed satisfactory performance (accuracy of 80%) in identifying whether the patient was high-sensitive or low-sensitive. In accordance with the training classification results, this study further confirmed that the features of PSD and FC with cubic SVM algorithm could predict pain sensitivity, and the neurophysiological data could be the pivotal signatures of pain perception processes [14]. Furthermore, this finding is in line with the increased attention of brain-based biomarkers in predictive modeling [38]. Combining multimodal parameters for prediction was suggested to be a compelling approach to pain prediction in clinical practice [39]. In general, the pain sensitivity classification and prediction model established in this study could eventually be applied in clinical practice and could objectively evaluate pain sensitivity without the presence of subjective ratings. Furthermore, although satisfactory accuracy (80%) of the validation, future investigations including the genetic factors [40, 41] or vital signs (heart rate variability or respiration) [42–44] might further improve the performance.

5.4 Limitations

This study has several limitations. First, this study confirmed that machine learning algorithms could classify and predict individuals with high-sensitivity and low-sensitivity. On the basis of these findings, in future, the

regression learning model might be used to examine varied degrees of pain sensitivity in larger samples other than just the classification of high- or low-sensitivity. Second, the generalizability of the present findings to pain sensitivity with respect to other sensory modalities (e.g., cold pain, punctate pain, or pressure pain) remains undetermined, which could be further investigated using a comparative study across sensory modalities. Third, the future investigations of this classification technique on the clinical applications are warranted including the discrimination between those experiencing from not experiencing actual pain, and the evaluation of pain severity. Finally, the predictive model presented in this study must be validated using a large dataset, eventually working toward clinical application.

6. Conclusions

Neural oscillations and intrinsic functional connectivity from resting-state EEG data could represent the underlying signatures of pain sensitivity. Accurate classification and prediction of pain sensitivity by using the SVM model led to considerable possibilities of objective evaluation of pain perception in clinical practice.

7. Author contributions

FJH, WTC and SJW conceived and design the work and wrote the article. FJH, WTC, LLHP, HYL, YFW, SPC, KLL and SJW acquired the data. FJH, WTC, LLHP, HYL, YFW, SPC, KLL and SJW analyzed the data and participated in the discussion and provided the comments. All of the authors have read and approved the manuscript.

8. Ethics approval and consent to participate

The Institutional Review Board of National Yang-Ming University approved the study protocol (YM108044F), and each participant provided written informed consent.

9. Acknowledgment

We would like to thank the study participants for actively participating. This work was supported by the Brain Research Center, National Yang Ming Chiao Tung University, from the Featured Areas Research Center Program within the framework of the Higher Education Sprout Project by the Ministry of Education of Taiwan.

10. Funding

This work was funded by the Ministry of Science and Technology of Taiwan (MOST 109-2314-B-075 -050 -MY2 to WT Chen, 108-2321-B-010-001, 108-2321-B-010-014-MY2, and 110-2321-B-010-005 to SJ Wang, and 108-2221-E-010-004 and 109-2221-E-003-MY2 to FJ Hsiao).

11. Conflict of interest

The authors declare no conflict of interest. SJW reports grants and personal fees from Norvatis Taiwan, personal fees from Daiichi-Sankyo, grants and personal fees from Eli-Lilly, personal fees from Allergan, personal fees from Pfizer, Taiwan, personal fees from Bayer, Taiwan, outside the submitted work.

12. References

[1] Raja SN, Carr DB, Cohen M, Finnerup NB, Flor H, Gibson S, *et al*. The revised International Association for the Study of Pain definition of pain: concepts, challenges, and compromises. Pain. 2020; 161: 1976–1982.

[2] Coghill RC, Eisenach J. Individual Differences in Pain Sensitivity: Implications for Treatment Decisions. Anesthesiology. 2003; 98: 1312–1314.

[3] Benedetti F, Vighetti S, Ricco C, Lagna E, Bergamasco B, Pinessi L, *et al*. Pain threshold and tolerance in Alzheimer's disease. Pain. 1999; 80: 377–382.

[4] Cole LJ, Farrell MJ, Duff EP, Barber JB, Egan GF, Gibson SJ. Pain sensitivity and fMRI pain-related brain activity in Alzheimer's disease. Brain. 2006; 129: 2957–2965.

[5] Mylius V, Engau I, Teepker M, Stiasny-Kolster K, Schepelmann K, Oertel WH, *et al*. Pain sensitivity and descending inhibition of pain in Parkinson's disease. Journal of Neurology, Neurosurgery & Psychiatry. 2009; 80: 24–28.

[6] Petzke F, Clauw DJ, Ambrose K, Khine A, Gracely RH. Increased pain sensitivity in fibromyalgia: effects of stimulus type and mode of presentation. Pain. 2003; 105: 403–413.

[7] Ashina S, Lipton RB, Bendtsen L, Hajiyeva N, Buse DC, Lyngberg AC, *et al*. Increased pain sensitivity in migraine and tension-type headache coexistent with low back pain: a cross-sectional population study. European Journal of Pain. 2018; 22: 904–914.

[8] Rolke R, Magerl W, Campbell KA, Schalber C, Caspari S, Birklein F, *et al*. Quantitative sensory testing: a comprehensive protocol for clinical trials. European Journal of Pain. 2006; 10: 77–88.

[9] Coghill RC, Sang CN, Maisog JM, Iadarola MJ. Pain Intensity Processing within the Human Brain: a Bilateral, Distributed Mechanism. Journal of Neurophysiology. 1999; 82: 1934–1943.

[10] Hsiao FJ, Chen WT, Liao KK, Wu ZA, Ho LT, Lin YY. Oscillatory Characteristics of Nociceptive Responses in the SII Cortex. Canadian Journal of Neurological Sciences. 2008; 35: 630–637.

[11] Furman AJ, Meeker TJ, Rietschel JC, Yoo S, Muthulingam J, Prokhorenko M, *et al*. Cerebral peak alpha frequency predicts individual differences in pain sensitivity. NeuroImage. 2018; 167: 203–210.

[12] Nickel MM, May ES, Tiemann L, Schmidt P, Postorino M, Ta Dinh S, *et al*. Brain oscillations differentially encode noxious stimulus intensity and pain intensity. NeuroImage. 2017; 148: 141–147.

[13] Furman AJ, Prokhorenko M, Keaser ML, Zhang J, Chen S, Mazaheri A, *et al*. Sensorimotor Peak Alpha Frequency is a Reliable Biomarker of Prolonged Pain Sensitivity. Cerebral Cortex. 2020; 30: 6069–6082.

[14] Hsiao FJ, Chen WT, Liu HY, Wang YF, Chen SP, Lai KL, *et al*. Individual pain sensitivity is associated with resting-state cor-

tical activities in healthy individuals but not in patients with migraine: a magnetoencephalography study. The Journal of Headache and Pain. 2020; 21: 133.
[15] Wager TD, Atlas LY, Lindquist MA, Roy M, Woo CW, Kross E. An fMRI-Based Neurologic Signature of Physical Pain. New England Journal of Medicine. 2013; 368: 1388–1397.
[16] Brown JE, Chatterjee N, Younger J, Mackey S. Towards a physiology-based measure of pain: patterns of human brain activity distinguish painful from non-painful thermal stimulation. PLoS ONE. 2011; 6: e24124.
[17] Huang G, Xiao P, Hung YS, Iannetti GD, Zhang ZG, Hu L. A novel approach to predict subjective pain perception from single-trial laser-evoked potentials. NeuroImage. 2013; 81: 283–293.
[18] Gruss S, Treister R, Werner P, Traue HC, Crawcour S, Andrade A, *et al*. Pain Intensity Recognition Rates via Biopotential Feature Patterns with Support Vector Machines. PLoS ONE. 2015; 10: e0140330.
[19] Tu Y, Zeng F, Lan L, Li Z, Maleki N, Liu B, *et al*. An fMRI-based neural marker for migraine without aura. Neurology. 2020; 94: e741–e751.
[20] Zhu B, Coppola G, Shoaran M. Migraine classification using somatosensory evoked potentials. Cephalalgia. 2019; 39: 1143–1155.
[21] Barry RJ, Rushby JA, Wallace MJ, Clarke AR, Johnstone SJ, Zlojutro I. Caffeine effects on resting-state arousal. Clinical Neurophysiology. 2005; 116: 2693–2700.
[22] Oostenveld R, Praamstra P. The five percent electrode system for high-resolution EEG and ERP measurements. Clinical Neurophysiology. 2001; 112: 713–719.
[23] Florin E, Baillet S. The brain's resting-state activity is shaped by synchronized cross-frequency coupling of neural oscillations. NeuroImage. 2015; 111: 26–35.
[24] Cheng CH, Wang PN, Mao HF, Hsiao FJ. Subjective cognitive decline detected by the oscillatory connectivity in the default mode network: a magnetoencephalographic study. Aging. 2020; 12: 3911–3925.
[25] Hsiao FJ, Wang SJ, Lin YY, Fuh JL, Ko YC, Wang PN, *et al*. Altered insula-default mode network connectivity in fibromyalgia: a resting-state magnetoencephalographic study. The Journal of Headache and Pain. 2017; 18: 89.
[26] Hsiao FJ, Wang YJ, Yan SH, Chen WT, Lin YY. Altered oscillation and synchronization of default-mode network activity in mild Alzheimer's disease compared to mild cognitive impairment: an electrophysiological study. PLoS ONE. 2013; 8: e68792.
[27] Babiloni C, Ferri R, Binetti G, Cassarino A, Forno G, Ercolani M, *et al*. Fronto-parietal coupling of brain rhythms in mild cognitive impairment: a multicentric EEG study. Brain Research Bulletin. 2006; 69: 63–73.
[28] Colclough GL, Woolrich MW, Tewarie PK, Brookes MJ, Quinn AJ, Smith SM. How reliable are MEG resting-state connectivity metrics? NeuroImage. 2016; 138: 284–293.
[29] Brookes MJ, Woolrich MW, Barnes GR. Measuring functional connectivity in MEG: a multivariate approach insensitive to linear source leakage. NeuroImage. 2012; 63: 910–920.
[30] Hipp JF, Hawellek DJ, Corbetta M, Siegel M, Engel AK. Large-scale cortical correlation structure of spontaneous oscillatory activity. Nature Neuroscience. 2012; 15: 884–890.
[31] Tadel F, Baillet S, Mosher JC, Pantazis D, Leahy RM. Brainstorm: a User-Friendly Application for MEG/EEG Analysis. Computational Intelligence and Neuroscience. 2011; 2011: 879716.
[32] Adler G, Gattaz WF. Pain perception threshold in major depression. Biological Psychiatry. 1993; 34: 687–689.
[33] Thompson T, Correll CU, Gallop K, Vancampfort D, Stubbs B. Is Pain Perception Altered in People with Depression? A Systematic Review and Meta-Analysis of Experimental Pain Research. The Journal of Pain. 2016; 17: 1257–1272.
[34] Sullivan MJ, Martel MO, Tripp DA, Savard A, Crombez G. Catastrophic thinking and heightened perception of pain in others. Pain. 2006; 123: 37–44.
[35] Weissman-Fogel I, Sprecher E, Pud D. Effects of catastrophizing on pain perception and pain modulation. Experimental Brain Research. 2008; 186: 79–85.
[36] Ploner M, Sorg C, Gross J. Brain Rhythms of Pain. Trends in Cognitive Sciences. 2017; 21: 100–110.
[37] Bushnell MC, Čeko M, Low LA. Cognitive and emotional control of pain and its disruption in chronic pain. Nature Reviews Neuroscience. 2013; 14: 502–511.
[38] Woo CW, Chang LJ, Lindquist MA, Wager TD. Building better biomarkers: brain models in translational neuroimaging. Nature Neuroscience. 2017; 20: 365–377.
[39] Lee J, Mawla I, Kim J, Loggia ML, Ortiz A, Jung C, *et al*. Machine learning-based prediction of clinical pain using multimodal neuroimaging and autonomic metrics. Pain. 2019; 160: 550–560.
[40] Kim H, Neubert JK, San Miguel A, Xu K, Krishnaraju RK, Iadarola MJ, *et al*. Genetic influence on variability in human acute experimental pain sensitivity associated with gender, ethnicity and psychological temperament. Pain. 2004; 109: 488–496.
[41] Norbury TA, MacGregor AJ, Urwin J, Spector TD, McMahon SB. Heritability of responses to painful stimuli in women: a classical twin study. Brain. 2007; 130: 3041–3049.
[42] Appelhans BM, Luecken LJ. Heart rate variability and pain: Associations of two interrelated homeostatic processes. Biological Psychology. 2008; 77: 174–182.
[43] Jafari H, Courtois I, Van den Bergh O, Vlaeyen JWS, Van Diest I. Pain and respiration: a systematic review. Pain. 2017; 158: 995–1006.
[44] Tracy LM, Koenig J, Georgiou-Karistianis N, Gibson SJ, Giummarra MJ. Heart rate variability is associated with thermal heat pain threshold in males, but not females. International Journal of Psychophysiology. 2018; 131: 37–43.

Keywords: Pain sensitivity; Resting-state EEG; Power spectral density; Functional connectivity; Machine learning; Support vector machine

Send correspondence to:

Fu-Jung Hsiao, Brain Research Center, National Yang-Ming Chiao-Tung University, 11221 Taipei, Taiwan, E-mail: fujunghsiao@gmail.com

Wei-Ta Chen, Brain Research Center, National Yang-Ming Chiao-Tung University, 11221 Taipei, Taiwan, School of Medicine, National Yang-Ming Chiao-Tung University, 11221 Taipei, Taiwan, Department of Neurology, Neurological Institute, Taipei Veterans General Hospital, 11217 Taipei, Taiwan, Department of Neurology, Keelung Hospital, Ministry of Health and Welfare, 20147 Keelung, Taiwan, E-mail: wtchen71@gmail.com